New Physics: Sae Mulli,
Vol. 69, No. 7, July 2019, pp. 690∼694
http://dx.doi.org/10.3938/NPSM.69.690

SERS-Based Sandwich Immunoassay for Alzheimer's Disease Biomarker Detection Using Antibody Conjugated Magnetic Nanoparticles

Seong Jin Back · Gyeong Bok Jung*
Department of Physics Education, Chosun University, Gwangju 61452, Korea

Yeron Lee · Jeunghee Park
Department of Advanced Materials Chemistry, Sejong University, Sejong 30019, Korea

(Received 2 April 2019 : revised 25 May 2019 : accepted 28 May 2019)

Surface-enhanced Raman scattering (SERS)-based immunoassays have been developed for fast and ultrasensitive detection of biomarkers. In this study, we report a SERS-based sandwich immunoassay for the detection of the Alzheimer's disease biomarker amyloidβ(Aβ). A method combining magnetic separation and SERS was developed to detection of Aβ. Gold-coated magnetic nanoparticles (Fe_3O_4@Au MNPs) were prepared by immobilizing anti-Aβ antibodies and was used in the separation and the concentration of the Aβ. Gold nanoparticles (Au NPs) were modified with detection antibodies, and antibody-conjugated Au NPs were labeled with 3, 3, diethylthiatricarbocyanine iodide (DTTC), as the SERS probes. The correlation between the Aβ concentration and the SERS signal was found to be linear within the range from 1 fM to 1 μM. As a result, we were able to detect Aβ with a much lower limit of 1 fM. This technique allows for straightforward SERS-based bioassays for the quantitative detection of biomarkers and has potential for clinical applications.

PACS numbers: 74.25.nd, 42.62.Be, 87.15.M−, 42.15. Eq, 81.05.−t
Keywords: Surface enhanced roman scattering (SERS), Alzheimer, Amyloid-β (Aβ), Biomarker, Nanoparticle

I. INTRODUCTION

Alzheimer's disease (AD) is a severe neurodegenerative disease of the brain that is characterized by a progressive destruction of memory and cognitive decline [1–5]. AD is predicted that there will be over 115 million individuals diagnosed with AD worldwide by 2050, which it is one of the biggest problems in the 21st century [6, 7]. Despite this issue, presently there is no cure and no definitive early diagnosis for AD. AD is pathologically characterized by a deposition of extracellular plaque composed of amyloid-β peptide (Aβ). Different assembled states of Aβ have been considered as important biomarkers for the diagnosis of AD [8–10]. Therefore, early diagnosis of possible AD biomarkers is crucial for society. The detection method of Aβ is based on measuring specific optical absorption such as the enzyme-linked immunosorbent assay (ELISA), which has been up to now the most practiced method [11,12]. However, this approach often requires a complicated sample preparation or multiple intermediate steps, which are costly and time-consuming.

Surface enhanced Raman scattering (SERS)-based immunoassay has attracted great interest as a powerful analytical technique, which provides the reduced susceptibility of Raman active compounds photobleaching, adaptability to high level multiplex applications, and is utilized in medicine as a diagnostic technique [13–17]. Furthermore, this technique has many advantages such as less water interference, non-destructive analysis, high sensitivity, and low detection limit [18–20]. The SERS

*E-mail: gbjung@chosun.ac.kr

immunoassay is the platform for detecting target antigens using metal nanoparticles. Recently, several studies have focused on the application of magnetic nanoparticles to SERS-based immunoassays [21–25]. The advantages of using magnetic nanoparticles are the higher capture efficiency due to the high surface-to-volume ratio, which can separate an analytes from samples, include faster reaction kinetics and minimize sample preparation.

In this study, we describe SERS-based sandwich immunoassay for highly sensitive Aβ detection based on SERS using antibody conjugated magnetic nanoparticles and gold nanoparticles as SERS probes.

II. EXPERIMENTAL METHODS

1. Materials

Citric acid ($C_6H_8O_7$, 99%) and trisodium-citrate ($C_6H_5Na_3O_7 \cdot 2H_2O$), tetrachloroauric acid trihydrate ($H[AuCl_4] \cdot 3H_2O$, 99.9%), iron(III) chloride hexahydrate ($FeCl_3 \cdot 6H_2O$), sodium acetate anhydrous ($C_2H_3NaO_2$), and polyethylenimine (PEI, MW: 10,000, 99%), HS-PEG-COOH (MW 3.5 kDa), diethylthiatricarbocyanine iodide (DTTC), N-hydroxy sulfosuccinimide sodium salt (sulfo-NHS), 1-ethyl-3-(3-dimethyl amino propyl)carbodiimide · HCl (EDC), and Tween 20, bovine serum albumin (BSA), Anti-β amyloid protein (1-40) antibody, Amyloid β protein fragment 1-40 were supplied by Sigma-Aldrich. All chemicals were used without further purification and Milli-Q water was used throughout.

2. Synthesis of Au NPs and Fe_3O_4@Au MNPs

Gold (Au) nanoparticle solutions were prepared by the standard citrate reduction method [26]. Briefly, 2.5 mL of a $H[AuCl_4]{\cdot}3H_2O$ solution (0.2% w/v) in 50 mL of water was heated to boiling and then 2 mL of sodium-citrate solution (1% w/v, containing 0.05% w/v citric acid) were added quickly under vigorous stirring. The solution was kept boiling for 5 min and was then allowed to cool down.

Magnetic Fe_3O_4 nanoparticles were prepared through a solvothermal reaction following a reported method in order to obtain a superparamagnetic (– 70 emu/g), sample [27]. Briefly, 2.7 g (0.026 mol) of $FeCl_3 \cdot 6H_2O$ and 7.2 g (0.087 mol) of sodium acetate were dissolved in 80 mL of ethylene glycol under magnetic stirring. The obtained homogeneous yellow solution was transferred to a Teflon-lined stainless-steel autoclave and sealed to heat at 200 °C for 8 h. The obtained black magnetite nanoparticles were washed with ethanol 6 times, and then dried in vacuum at 60 °C for 12 h. Then, 50 mg of as-prepared Fe_3O_4 nanoparticles was functionalized with polyethylenimine (PEI) by suspending them in 100 mL of 5.0 mg/mL positively charged PEI solution, PEI supplies amino groups around a Fe_3O_4 nanoparticle. Then Au nanoparticles (in solution) were mixed with the amino-functionalized Fe_3O_4 nanoparticles to produce the Fe_3O_4@Au nanoparticles.

3. Antibody conjugation to Fe_3O_4@Au MNPs and Au NPs

A scheme of the stepwise immunoassay design process of the nanoparticle preparation and its selective detection of Aβ is shown in Fig. 1. Fig. 1(a) shows the conjugation of the as synthesized Fe_3O_4@Au NPs to capture antibody. The surface of gold-coated magnetic nanoparticles was modified with 1μM HS-PEG-COOH. To active the carboxyl groups on the Fe_3O_4@Au MNPs surface for covalent conjugation, freshly prepared EDC and sulfo-NHS were mixed. The activated nanoparticles were collected using permanent magnet and washed twice with K_2CO_3 solution. Then, 4 μL of capture antibody was added and incubated at 4 °C overnight. In order to avoid the occurrence of non-specific interaction, 1% BSA solution was added for 2 h to block the active groups. The NPs were washed twice with PBS buffer and then resuspended in PBS solution containing 1% BSA and stored at 4 °C until use.

The Au NPs were used as SERS probes by assembling DTTC, and conjugated with a detection antibody. As shown in Fig. 1(b), the surface of the gold nanoparticles was modified with 1 μM HS-PEG-COOH and 0.01% Tween 20, which have free carboxyl groups on the surface

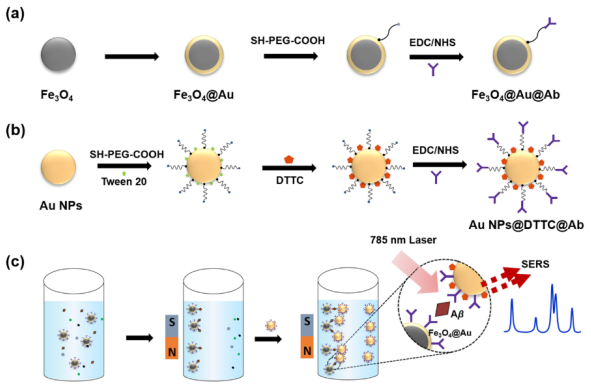

Fig. 1. (Color online) Schematic illustration of SERS-based sandwich immunoassay for amyloid- (A). (a) the conjugation of Fe3O4@Au MNPs to the capture antibody, (b) the conjugation of Au NPs to the detection antibody, and (c) the operating principle of SERS immunoassay for A detection.

of the nanoparticles. Then 300 μL of 25 μM DTTC solution was added to the pegylated Au NPs solution to synthesize Raman encoded NPs. To improve the stability of the NPs 30 μL 1 mM mPEG-SH solution was added and continuously sonicated for another 30 min. After that, the mixture was centrifuged at 15,000 rpm for 10 min and resuspended in K_2CO_3 solution (3 mM, pH 8.5). For surface activation over carboxyl groups, NPs were treated 25 μM EDC and sulfo-NHS. Excess EDC and sulfo-NHS were removed from the activated NPs through centrifugation (15,000 rpm, 10 min) and resuspension in K_2CO_3 solution. Then the activated NPs were mixed with 4 μL of detection antibody and incubated at 4 °C overnight. Unreacted groups on the NPs surface were blocked with 1% BSA solution for 2h. After the washing procedure, antibody immobilized Au NPs were dispersed in PBS solution containing 1% BSA and stored at 4 °C prior to use.

4. Preparation of sandwich immunoassay

The Aβ solution with the concentrations in a range from 1 fM to 1 μM was obtained by a serial dilution with PBS. The capture antibody coated Fe_3O_4@Au MNPs were added into each Aβ solution and incubated for 30 min at 37 °C under gentle shaking. After immune capture of the target Aβ, the immune complexes were isolated with a magnet and washed twice with PBS buffer. Then, 50 μL of the DTTC encoded Au NPs SERS probes were added and incubated for 30 min at 37 °C with gentle shaking. Finally, the resultant sandwich complex was collected with a magnet and washed three times with PBS solution, resuspended in 5 μL of deionized water and then transferred to a glass for SERS measurements.

5. Characterization of NPs and SERS measurement

The transmission electron microscopy (TEM) imaging of NPs was conducted using a high-voltage TEM (HVEM, JEOL JEM ARM 1300S, 1.25 MV). The absorption spectrum of NPs was measured using a UV–vis spectrophotometer (Optizen 3220UV; MECASYS). Raman spectra were recorded on an XperRam F1.4 (Nanobase Inc., Seoul, Korea) equipped with a 785 nm diode laser source (7 mW before sample), numerical aperture of 0.4, and a TE-cooled CCD detector. All Raman measurements were recorded with an accumulation time of 5 s in the 600-1800 cm^{-1} range. Baseline correction was performed for all measurement.

III. RESULTS AND DISCUSSION

Figure 1 shows the operating principle of SERS-based sandwich immunoassay developed for magnetic capture and SERS detection of target antigen Aβ. The gold coated magnetic nanoparticles (Fe_3O_4@Au MNPs) were prepared by immobilizing anti-Aβ antibodies and utilized as the separation and enrichment of the Aβ. Gold nanoparticles (Au NPs) were modified with antibody-conjugated Au NPs labeled with 3, 3, diethylthia- tricarbocyanine iodide (DTTC), which used as a SERS probes. The Aβ antibody conjugated Au NPs and Fe_3O_4@Au MNPs would form the sandwich immune complex in the presence of the target biomarker Aβ.

Gold nanoparticles (Au NPs) and gold-coated magnetic nanoparticles (Fe_3O_4@Au MNPs) were produced for SERS labelling and magnetic separation, respectively. TEM images of Au NPs and Fe_3O_4@Au MNPs

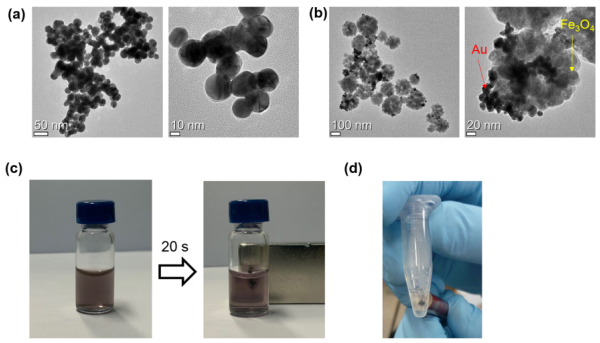

Fig. 2. (Color online) Characterization of the properties of NPs. TEM images of (a) Au NPs and (b) Fe_3O_4@Au MNPs. Magnetic separation behavior of (c) Fe_3O_4@Au MNPs and (d) Fe_3O_4@Au@Ab in the solution.

are shown in Fig. 2(a) and 2(b), indicating that the average diameters are 15 nm and 80 nm, respectively. Figure 2(c) and 2(d) show the magnetic separation behavior of Fe_3O_4@Au MNPs and Fe_3O_4@Au@Ab in the solution, which it was completely separated from the solution within 20s when an external magnetic field was applied. This result indicates that the MNPs could be used for the rapid separation and enrichment of analytes.

Figure 3 shows the extinction spectra of the Au NPs (black line), DTTC-adsorbed Au NPs (red line) and DTTC-adsorbed Au NPs conjugated with anti-Aβ (blue line). The characteristic UV-vis plasmon peak of the Au NPs is at 552 nm. The DTTC-adsorbed Au NPs and DTTC-adsorbed Au NPs conjugated with anti-Aβ antibody bring on a red shift of the plasmon band to 557 nm, and peak broadening was observed in around of 653 nm. Red shifting of the plasmon peak is a common optical property of Au NPs following surface immobilization and is dependent upon size, shape, and aggregation etc [28,29].

The SERS detection is based on a characteristic feature of the Raman probe and then quantified by its intensity. We investigated the relationship between SERS intensity and Aβ concentration. Figure 4(a) shows the SERS spectra for Aβ assays conducted by using Raman probe constructed from Au NPs. The SERS signal intensity of DTTC increases significantly with an increasing Aβ concentration. The SERS intensity of the DTTC major peak at 1236 cm^{-1} was investigated. Figure 4(b) shows the sensitivity curves obtained by plotting the 1236 cm^{-1} band intensity as a function of the logarithm of Aβ concentration. The calibration curve in

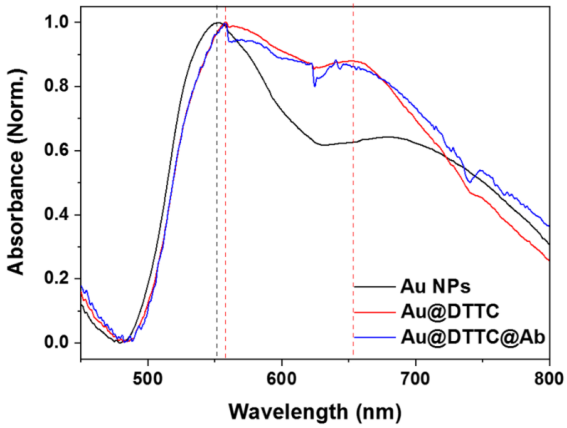

Fig. 3. (Color online) UV-vis absorption spectra of Au NPs (black line), DTTC-adsorbed Au NPs (red line) and DTTC-adsorbed Au NPs conjugated with anti-A antibody (blue line).

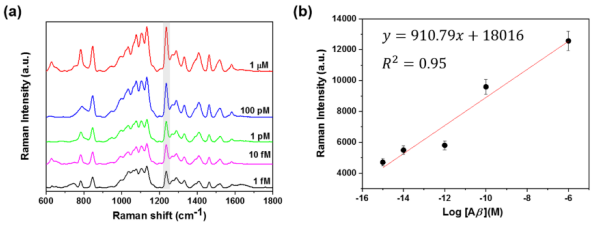

Fig. 4. (Color online) (a) SERS spectra obtained from the sandwich immunoassay with various concentration of Aβ. (b) Plot of the Raman intensity at 1236 cm^{-1} as a function of the logarithmic concentration of Aβ.

Fig. 4(b) displays a good linear relationship between the intensity of the SERS peak at 1236 cm^{-1} and the Aβ concentration in the range from 1 μM to 1 fM. The linear regression equation was $y = 910.79x + 18016$ with a correlation coefficient (R^2) of 0.95. The detection limit was much lower than 1 fM. In conventional biosensor such as ELISA, the detection limit of Aβ concentration is about pM. The proposed SERS-based sandwich immunoassay method showed 1,000 times higher sensitivity than ELISA method. Therefore, we consider that this technique could be a useful tool for the early diagnosis of Alzheimer's disease. These results indicated that this technique can be attributed to the separation and enrichment capability of the magnetic nanoparticles, and the significant enhancement induced by the hot spot formation in the coupled Fe_3O_4@Au MNPs and Au NPs nanostructures.

IV. CONCLUSIONS

We have developed a SERS-based sandwich immunoassay for fast and sensitive detection of Aβ by using of Fe_3O_4@Au MNPs and Au NPs. Antibody-conjugated DTTC-labeled Au NPs were served as the SERS probes. The Fe_3O_4@Au MNPs were utilized as the capture and enrichment platform of Aβ. As a result, the proposed sandwich type SERS immunoassay was able to detect with high sensitivity the Aβ, possessing the detection of much lower of 1 fM and a wide dynamic linear range of 1 fM to 1 M. Furthermore, the proposed method using magnetic immunoassay is offers rapid detection using a simple and cost-effective. Therefore, this technique might be a useful tool for the early diagnosis of Alzheimer's disease and in point-of-care test.

ACKNOWLEDGEMENTS

This work was supported by Basic Science Research Program through the National Research Foundation of Korea (NRF) funded by the Ministry of Education (NRF-2016R1D1A3B03931548).

REFERENCES

[1] R. Brookmeyer, E. Johnson, K. Ziegler-Graham and M. H. Arrighi, Alzheimer's Dementia **3**, 186 (2007).
[2] T. Hartmann, S. C. Bieger, B. Brühl and P. J. Tienari *et al.*, Nat. Med. **3**, 1016 (1997).
[3] G. Bu, Nat. Rev. Neurosci. **10**, 333 (2009).
[4] S. T. Ferreira, W. L. Klein, Neurobiol. Learn. Mem. **96**, 529 (2011).
[5] H. Amiri, K. Saeidi, P. Borhani and A. Manafirad ACS Chem. Neurosci. **4**, 1417 (2013).
[6] R. Brookmeyer, E. Johnson, K. Ziegler-Graham and M. H. Arrighi, Alzheimer's Dementia **3**, 186 (2007).
[7] S. S. Sisodia, J. Clin. Invest. **104**, 1169 (1999).
[8] J. Wiltfang, P. Lewczuk and M. Otto, Nervenarzt **87**, 1305 (2016).
[9] Y. Zhou, L. Liu, Y. Hao and M. Xu, Chem. Asian J. **11**, 805 (2016).
[10] C. Humpel, Trends Biotechnol. **29**, 26 (2011).
[11] N. Mattsson, U. Andreasson, S. Persson and M. C. Carrillo *et al.*, Alzheimer's Dementia **9**, 251 (2013).
[12] N. L. Bastard, P. P. D. Deyn and S. Engelborghs, Clin. Chem. **61**, 734 (2015).
[13] J. Ni, R. J. Lipert, G. B. Dawson and M. D. Porter, Anal. Chem. **71**, 4903 (1999).
[14] M. Li, S. K. Cushing, J. Zhang, S. Suri and R. Evans *et al.*, ACS Nano **6**, 4967 (2013).
[15] A. Kamińska, E. Witkowska, K. Winkler and I. Dziecielewski *et al.*, Biosens. Bioelectron. **66**, 461 (2015).
[16] K. Karn-orachai, K. Sakamoto, R. Laocharoensuk and S. Bamrungsap *et al.*, RSC Adv. **6**, 97791 (2016).
[17] N. Narayanan, V. Karunakaran, W. Paul and K. Venugopal *et al.*, Biosens. Bioelectron. **70**, 145 (2015).
[18] L. Wu, Z. Wang, K. Fan and S. Zong *et al.*, Small **11**, 2798 (2015).
[19] S. L. Kleinman, E. Ringe, N. Valley and K. L. Wustholz *et al.*, J. Am. Chem. Soc. **133**, 4115 (2011).
[20] D. -K. Lim, K. -S. Jeon, H. M. Kim and J. -M. Nam *et al.*, Nat. Mater. **9**, 60 (2010).
[21] Z. Rong, C. Wang, J. Wang and D. Wang *et al.*, Biosens. Bioelectron. **84**, 15 (2016).
[22] J. Neng, M. H. Harpster, W. C. Wilson and P. A. Johnson, Biosens. Bioelectron. **41**, 316 (2013).
[23] C. Song, L. Min, N. Zhou and Y. Yang *et al.*, ACS Appl. Mater. Interfaces. **6**, 21842 (2014).
[24] P. Zhao, H. -X. Li, D. -W. Li and Y. -J. Hou *et al.*, Talanta **198**, 527 (2019).
[25] J. Wang, X. Wu, C. Wang and Z. Rong *et al.*, ACS Appl. Mater. Interfaces. **8**, 19958 (2016).
[26] C. Ziegler, A. Eychmüller, J. Phys. Chem. C **115**, 4502 (2011).
[27] H. Deng, X. Li, Q. Peng and X. Wang *et al.*, Angew. Chem. Int. Ed. Engl. **44**, 2782 (2005).
[28] S. Link, M. A. El-Sayed, J. Phys. Chem. B **103**, 4212 (1999).
[29] S. Zeng, K. -T. Yong, I. Roy and X. -Q. Dinh *et al.*, Plasmonics **6**, 491 (2011).